

Simulating and comparing the quantum and classical mechanically motion of two hydrogen atoms

Hui-hui Miao*

*Faculty of Computational Mathematics and Cybernetics,
Lomonosov Moscow State University, Vorobyovy Gory 1, Moscow, Russia*

(Dated: June 10, 2024)

A comprehensive comparison of quantum evolution between the quantum and classical mechanically motion of nuclei in a finite-dimensional quantum chemistry model is presented. A modified version of Tavis–Cummings–Hubbard model with two two-level artificial atoms in optical cavities is described for simulating the association and dissociation of neutral hydrogen molecule. The initial circumstances that led to the formation and decomposition of neutral hydrogen molecule are discussed. The dissipative process of Markovian open system is simulated through solving quantum master equation — Lindbladian. The motion of these two atoms (nuclei) both quantum and classical mechanically is compared. In quantum form, nuclei’s mobility is portrayed by tunneling effect of nuclei. And we describe the effect of the classical motion of nuclei on the interaction within the system by fluctuation of strengths. Consideration is also given to the dark state, which is produced along with the dissociation process and has a non-negligible impact on the final result of the evolution.

Keywords: neutral hydrogen molecule, finite-dimensional QED, dark state, quantum motion, classical motion.

I. INTRODUCTION

Thanks to the improvement of supercomputing capabilities, the ability to simulate chemical reactions has led to an increased interest in mathematical modeling of predictive modeling of chemistry. Numerous theoretical articles, such as those in [1–9], have recently aroused this interest. The modeling of chemical reactions related to hydrogen is one of the main objectives of chemical modeling, namely the association-dissociation reaction of the cation H_2^+ [1, 2], the positive hydrogen peroxide ion OH^+ in a thermal bath [6] and the neutral hydrogen molecule H_2 [7–9]. In our preliminary work on the association-dissociation model of neutral hydrogen molecule [7], the initial circumstances that led to the formation of H_2 and the effects of temperature variation on quantum evolution are studied. However, there are still many other aspects of this model that need to be further studied. The quantum and classical mechanically motion of nuclei in Markovian open system is the focus of this paper.

Models of quantum electrodynamics (QED) offer a unique physical framework for studying the interaction of light and matter, and have led to many famous studies, such as, quantum Rabi model (QRM) [10, 11], Dicke model [12], Hopfield model [13], Jaynes–Cummings model (JCM) [14], Tavis–Cummings model (TCM) [15], ultrastrong coupling (USC) and deep strong coupling (DSC) models [16–21]. The Tavis–Cummings–Hubbard model (TCHM) [22], which is a fundamental contribution to this paper, is generalizations of TCM to multiple cavities coupled by optical fibres. TCHM is one of the more

straightforward strong coupling (SC) models, of which regime occurs when

$$\eta = \max\left(\frac{g}{\hbar\omega_c}, \frac{g}{\hbar\omega_a}\right) < 0.1 \quad (1)$$

where $\hbar = h/2\pi$ — reduced Planck constant or Dirac constant, g — coupling strength, ω_c — cavity frequency and ω_a — atomic frequency. Because it is very easy to implement in the laboratory, many studies have been conducted recently in the field of SC models, including those on phase transitions [23, 24], quantum many-body phenomena [25], quantum gates [26, 27], entropy [28], quantum discord [29], dark states [30–38], etc [39–45].

In this paper, we propose a modified version of finite-dimensional TCHM and compare difference of quantum evolution between the quantum and classical mechanically motion of nuclei. We discuss the effect of different initial circumstances on the result of association-dissociation process of neutral hydrogen molecule. The Markovian dissipative process is obtained through solving quantum master equation (QME) [46–48]. Dark state is also the focus in this paper. In addition, a so-called precise time step integration method (PTSIM) is introduced to compute matrix exponential.

This paper is organized as follows. After introducing the association-dissociation model of the neutral hydrogen molecule in Sec. IIA, we introduce the quantum master equation in sec. IIB. We take into account the interaction between the system and the external environment in Sec. IIC. And we introduce both the quantum and classical motion of nuclei in. Sec. IID. We offer a numerical technique to solve quantum master equation in Sec. III. We present the results of our numerical simulations in Sec. IV. Some brief comments on our results and extension to future work in Sec. V close out the paper. Some technical details are included in Appendices A~C.

* Correspondence to: Vorobyovy Gory 1, Moscow, 119991, Russia.
E-mail address: hhmiao@cs.msu.ru (H.-H. Miao)

II. THE ASSOCIATION-DISSOCIATION MODEL OF NEUTRAL HYDROGEN MOLECULE

The association-dissociation model of the neutral hydrogen molecule, studied in detail in our previous work on quantum evolution [7, 8]. In this paper, we directly quote this model and study the quantum and classical mechanically motion of two hydrogen atoms.

A. The target model

The schematic diagram of the target model is shown in Fig. 1. In the model, each energy level, both atomic and molecular, is split into two levels: spin up \uparrow and spin down \downarrow . For each level there must be no more than one electron according to Pauli exclusion principle [49]. Hybridization of atomic orbitals (AO) and formation of molecular orbitals (MO) are shown in Fig. 1 (a), where molecular ground orbital (bonding orbital) takes the form

$$\Phi_0 = \frac{1}{\sqrt{2}} (0_1 + 0_2) \quad (2)$$

$$|\Psi\rangle_{\mathcal{C}} = |p_1\rangle_{\omega^\uparrow} |p_2\rangle_{\omega^\downarrow} |p_3\rangle_{\Omega^\uparrow} |p_4\rangle_{\Omega^\downarrow} |p_5\rangle_{\Omega^s} |l_1\rangle_{at_1}^\uparrow |l_2\rangle_{or_0}^\downarrow |l_3\rangle_{at_1}^\uparrow |l_4\rangle_{or_{-1}}^\downarrow |l_5\rangle_{at_2}^\uparrow |l_6\rangle_{or_0}^\downarrow |l_7\rangle_{at_2}^\uparrow |l_8\rangle_{or_{-1}}^\downarrow |k\rangle_n \quad (4)$$

where $p_{i,i \in \{1,2,\dots,5\}}$ is the number of photons, here $\omega^\uparrow, \omega^\downarrow$ are the modes of photon for electron transition between molecular orbitals, $\Omega^\uparrow, \Omega^\downarrow$ are the modes of photon for electron transition between atomic orbitals and Ω^s is the mode of photon for spin-flip in atomic system. In this paper, we suppose that every type of photon has a sufficiently large wavelength to interact with an electron located in any cavity. $l_{i,i \in \{1,2,\dots,8\}}$ describes orbital state: $l_i = 1$ — the orbital is occupied by one electron, $l_i = 0$ — the orbital is freed. The states of the nuclei are denoted by $|k\rangle_n$: $k = 0$ — state of nuclei, gathering together in one cavity, $k = 1$ — scattering in different cavities.

The coupled-system Hamiltonian of the association-dissociation model with consideration of rotating wave approximation (RWA, see Appx. A) is expressed by the total energy operator

$$H = H_{\mathcal{A}} + H_{\mathcal{D}} + H_{tun} + H_{spin} \quad (5)$$

$H_{\mathcal{A}}$ denotes the associative Hamiltonian and takes the following form

$$\begin{aligned} H_{\mathcal{A}} = & \left\{ \hbar\omega^\uparrow a_{\omega^\uparrow}^\dagger a_{\omega^\uparrow} + \hbar\omega^\downarrow a_{\omega^\downarrow}^\dagger a_{\omega^\downarrow} \right. \\ & + \hbar\omega^\uparrow \sigma_{\omega^\uparrow}^\dagger \sigma_{\omega^\uparrow} + \hbar\omega^\downarrow \sigma_{\omega^\downarrow}^\dagger \sigma_{\omega^\downarrow} \\ & + g_{\omega^\uparrow} \left(a_{\omega^\uparrow}^\dagger \sigma_{\omega^\uparrow} + a_{\omega^\uparrow} \sigma_{\omega^\uparrow}^\dagger \right) \\ & \left. + g_{\omega^\downarrow} \left(a_{\omega^\downarrow}^\dagger \sigma_{\omega^\downarrow} + a_{\omega^\downarrow} \sigma_{\omega^\downarrow}^\dagger \right) \right\} \sigma_n \sigma_n^\dagger \end{aligned} \quad (6)$$

And molecular excited orbital (antibonding orbital) takes the form

$$\Phi_1 = \frac{1}{\sqrt{2}} (0_1 - 0_2) \quad (3)$$

where Φ_0 is molecular ground orbital, Φ_1 is molecular excited orbital, 0_1 is excited orbital of the first nucleus, 0_2 is excited orbital of the second nucleus. Possible only for atomic excited orbitals is orbital hybridization. Hybridization is impossible for the atomic ground orbitals -1_1 and -1_2 . The electrons will be bound in the potential wells that each nucleus creates around itself. The formation of H_2 caused by the association reaction of two hydrogen atoms, accompanied by orbital hybridization and covalent bond formation, is depicted in panel Fig. 1 (b). The decomposition of H_2 caused by the dissociation reaction of these hydrogen atoms, accompanied by orbital de-hybridization and covalent bond breaking, is depicted in panel Fig. 1 (c).

We introduce the second quantization [50, 51] for describing the Hilbert space. As a result, the entire system's Hilbert space for quantum states is \mathcal{C} and takes the following form

where $\sigma_n \sigma_n^\dagger$ verifies that nuclei are close. $\hbar = h/2\pi$ is the reduced Planck constant. $g_{\omega^\uparrow, \downarrow}$ is the coupling strength between the photon mode $\omega^{\uparrow, \downarrow}$ (with annihilation and creation operators $a_{\omega^{\uparrow, \downarrow}}$ and $a_{\omega^{\uparrow, \downarrow}}^\dagger$, respectively) and the electrons in the molecule (with excitation and relaxation operators $\sigma_{\omega^{\uparrow, \downarrow}}^\dagger$ and $\sigma_{\omega^{\uparrow, \downarrow}}$, respectively). $H_{\mathcal{D}}$ denotes the dissociative Hamiltonian and takes the following form

$$\begin{aligned} H_{\mathcal{D}} = & \left\{ \hbar\Omega^\uparrow a_{\Omega^\uparrow}^\dagger a_{\Omega^\uparrow} + \hbar\Omega^\downarrow a_{\Omega^\downarrow}^\dagger a_{\Omega^\downarrow} \right. \\ & + \sum_{i=1,2} \left(\hbar\Omega^\uparrow \sigma_{\Omega^\uparrow, i}^\dagger \sigma_{\Omega^\uparrow, i} + \hbar\Omega^\downarrow \sigma_{\Omega^\downarrow, i}^\dagger \sigma_{\Omega^\downarrow, i} \right) \\ & + \sum_{i=1,2} \left[g_{\Omega^\uparrow} \left(a_{\Omega^\uparrow}^\dagger \sigma_{\Omega^\uparrow, i} + a_{\Omega^\uparrow} \sigma_{\Omega^\uparrow, i}^\dagger \right) \right. \\ & \left. \left. + g_{\Omega^\downarrow} \left(a_{\Omega^\downarrow}^\dagger \sigma_{\Omega^\downarrow, i} + a_{\Omega^\downarrow} \sigma_{\Omega^\downarrow, i}^\dagger \right) \right] \right\} \sigma_n^\dagger \sigma_n \end{aligned} \quad (7)$$

where i denotes index of atoms, and $g_{\Omega^\uparrow, \downarrow}$ is the coupling strength between the photon mode $\Omega^{\uparrow, \downarrow}$ and the electrons in the atom. H_{tun} denotes the quantum tunnelling effect between $H_{\mathcal{A}}$ and $H_{\mathcal{D}}$, and takes the following form

$$\begin{aligned} H_{tun} = & \zeta_2 \sigma_{\omega^\uparrow}^\dagger \sigma_{\omega^\uparrow} \sigma_{\omega^\downarrow}^\dagger \sigma_{\omega^\downarrow} (\sigma_n^\dagger + \sigma_n) \\ & + \zeta_1 \sigma_{\omega^\uparrow} \sigma_{\omega^\uparrow}^\dagger \sigma_{\omega^\downarrow} \sigma_{\omega^\downarrow} (\sigma_n^\dagger + \sigma_n) \\ & + \zeta_1 \sigma_{\omega^\uparrow}^\dagger \sigma_{\omega^\uparrow} \sigma_{\omega^\downarrow} \sigma_{\omega^\downarrow}^\dagger (\sigma_n^\dagger + \sigma_n) \\ & + \zeta_0 \sigma_{\omega^\uparrow} \sigma_{\omega^\uparrow}^\dagger \sigma_{\omega^\downarrow} \sigma_{\omega^\downarrow}^\dagger (\sigma_n^\dagger + \sigma_n) \end{aligned} \quad (8)$$

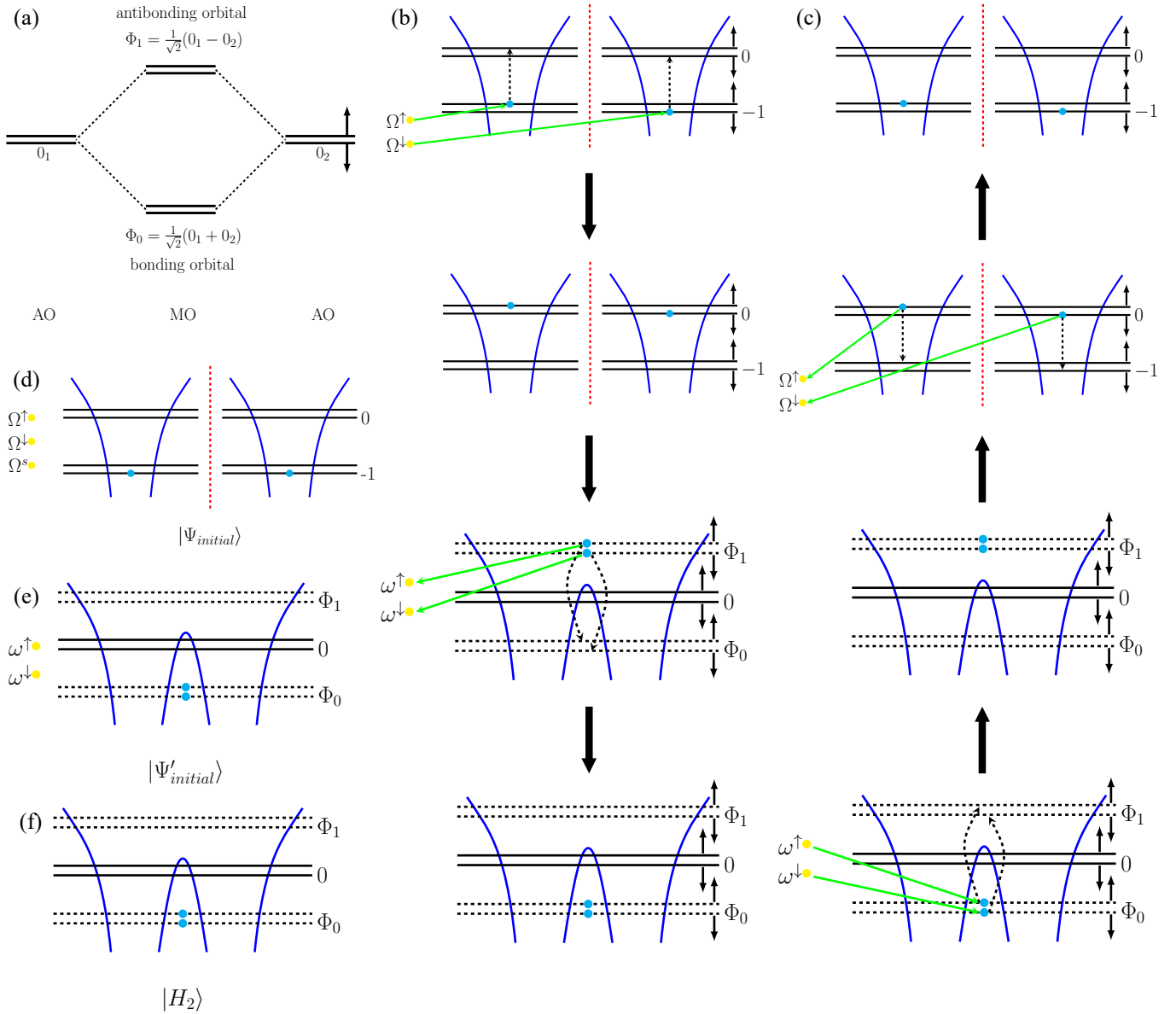


FIG. 1. (online color) *The association-dissociation model of neutral hydrogen molecule.* Schematic diagram of the hybridization of the excited orbitals of two atoms to form a molecular excited orbital (antibonding orbital) and a ground orbital (bonding orbital) is shown in panel (a). Panel (b) displays the association reaction of H_2 . Two electrons in the atomic ground orbital -1 with significant gaps between their nuclei, which correspond to two distinct spin directions, absorb respectively photons with modes Ω^\uparrow or Ω^\downarrow , before rising to the atomic excited orbital 0. The potential barrier between the two potential wells decreases when nuclei from different cavities come together in one cavity due to the quantum tunnelling effect. Since the two electrons are in atomic excited orbitals, the atomic orbitals are hybridized into molecular excited orbitals, and the electrons are released on the molecular excited orbital Φ_1 . Then, two electrons quickly emit photons with the modes ω^\uparrow or ω^\downarrow , respectively, and fall to the molecular ground orbital Φ_0 . Stable molecule is formed. The dissociation process of hydrogen molecule, shown in panel (c), is the reverse process of the association process. The initial state $|\Psi_{initial}\rangle$, in which two atoms are in different cavities, is depicted in panel (d). The initial state $|\Psi'_{initial}\rangle$, in which two atoms are in the same cavity and form a molecule, is depicted in panel (e). The state of stable hydrogen molecule $|H_2\rangle$ is shown in panel (f), where two electrons fall to the ground orbital. In panels (b)~(f), the blue and yellow dots, respectively, stand for electrons and photons. The vertical red dashed line indicates a significant distance between the nuclei, that is to say, the two nuclei are located in different optical cavities.

where $\sigma_{\omega\uparrow}^\dagger\sigma_{\omega\uparrow}\sigma_{\omega\downarrow}^\dagger\sigma_{\omega\downarrow}$ verifies that two electrons with different spins are at orbital Φ_1 with large tunnelling intensity ζ_2 ; $\sigma_{\omega\uparrow}\sigma_{\omega\uparrow}^\dagger\sigma_{\omega\downarrow}^\dagger\sigma_{\omega\downarrow}$ verifies that electron with \uparrow is at orbital Φ_0 and electron with \downarrow is at orbital Φ_1 , with low tunnelling intensity ζ_1 ; $\sigma_{\omega\uparrow}^\dagger\sigma_{\omega\uparrow}\sigma_{\omega\downarrow}\sigma_{\omega\downarrow}^\dagger$ verifies that electron with \uparrow is at orbital Φ_1 and electron with \downarrow is at orbital Φ_0 , with low tunnelling intensity ζ_1 ; $\sigma_{\omega\uparrow}\sigma_{\omega\uparrow}^\dagger\sigma_{\omega\downarrow}\sigma_{\omega\downarrow}^\dagger$ verifies that two electrons with different spins are at orbital Φ_0 with tunnelling intensity ζ_0 , which equal to 0. H_{spin} denotes the electron spin transition and takes the following form

$$H_{spin} = \hbar\Omega^s a_{\Omega^s}^\dagger a_{\Omega^s} + \hbar\Omega^s \sum_{i=1,2} \sigma_{\Omega^s,i}^\dagger \sigma_{\Omega^s,i} + g_{\Omega^s} \sum_{i=1,2} \left(a_{\Omega^s}^\dagger \sigma_{\Omega^s,i} + a_{\Omega^s} \sigma_{\Omega^s,i}^\dagger \right) \quad (9)$$

where i denotes index of atoms, and g_{Ω^s} is the coupling strength between the photon mode Ω^s and the electrons in the atom. The association-dissociation model is introduced with spin photons with mode Ω^s in this section, allowing for transitions between \uparrow and \downarrow . The Pauli exclusion principle, which prohibits the presence of electrons with the same spin at the same energy level, must be carefully followed by electron spins. We agree that an electron spin transition is only possible if the electrons are in the atomic states corresponding to $|1\rangle_n$. Electron spin transition is forbidden when electrons are in molecular states corresponding to $|0\rangle_n$, which contravenes Pauli exclusion principle.

Details of all operators used in Eqs. (6)~(9) are shown in Appx. B.

B. Quantum master equation

The dynamics of system is described by solving the QME in the Markovian approximation for the density operator ρ of the system

$$i\hbar\dot{\rho} = [H, \rho] + iL(\rho) \quad (10)$$

where $[H, \rho] = H\rho - \rho H$ is the commutator. We have a graph \mathcal{K} of the potential photon dissipations between the states that are permitted. The edges and vertices of \mathcal{K} represent the permitted dissipations and the states, respectively. Similar to this, \mathcal{K}' is a graph of potential photon influxes that are permitted. $L(\rho)$ is as follows

$$L(\rho) = \sum_{k \in \mathcal{K}} L_k(\rho) + \sum_{k' \in \mathcal{K}'} L_{k'}(\rho) \quad (11)$$

where $L_k(\rho)$ is the standard dissipation superoperator corresponding to the jump operator A_k and taking as an argument on the density matrix ρ

$$L_k(\rho) = \gamma_k \left(A_k \rho A_k^\dagger - \frac{1}{2} \left\{ \rho, A_k^\dagger A_k \right\} \right) \quad (12)$$

where $\left\{ \rho, A_k^\dagger A_k \right\} = \rho A_k^\dagger A_k + A_k^\dagger A_k \rho$ is the anticommutator. The term γ_k refers to the overall spontaneous emission rate for photons for $k \in \mathcal{K}$ caused by photon leakage from the cavity to the external environment. Similarly, $L_{k'}(\rho)$ is the standard influx superoperator, having the following form

$$L_{k'}(\rho) = \gamma_{k'} \left(A_k^\dagger \rho A_k - \frac{1}{2} \left\{ \rho, A_k A_k^\dagger \right\} \right) \quad (13)$$

The total spontaneous influx rate for photon for $k' \in \mathcal{K}'$ is denoted by $\gamma_{k'}$.

C. Thermally stationary state

As a mixed state with a Gibbs distribution of Fock components, we define the stationary state of a field with temperature T as follows

$$\mathcal{G}(T)_f = c \sum_{p=0}^{\infty} \exp\left(-\frac{\hbar\omega_c p}{KT}\right) |p\rangle\langle p| \quad (14)$$

where K is the Boltzmann constant, c is the normalization factor, p is the number of photons, ω_c is the photonic mode. The notation $\gamma_{k'}/\gamma_k = \mu$ is presented. Since the temperature would otherwise be endlessly high and the state $\mathcal{G}(T)_f$ would not be normalizable, the state will then only exist at $\mu < 1$ [52]. The probability of the photonic Fock state $|p\rangle$ at temperature T is proportional to $\exp\left(-\frac{\hbar\omega_c p}{KT}\right)$. In our model, we assume

$$\mu = \exp\left(-\frac{\hbar\omega_c}{KT}\right) \quad (15)$$

from where $T = \frac{\hbar\omega_c}{K \ln(1/\mu)}$.

D. Quantum and classical motion of nuclei

The three-dimensional surface diagram, shown in Fig. 2, intuitively shows how the double potential well around nuclei alters depending on how close or how far away they are. We propose two ways in which hydrogen nuclei can move:

- Quantum motion of nuclei. In this way, the nuclei use the quantum tunneling effect to move instantly between the optical cavities. As shown in Fig. 2 (a), the two nuclei are located in different optical cavities. At this time, the orbitals associated with each nucleus remain atomic, and all the interaction forces involving molecular orbitals do not exist, that is, $g_{\omega\uparrow,\downarrow} = 0$, and only the interaction forces $g_{\Omega\uparrow,\downarrow,s}$ involving atomic orbitals are retained. As shown in Fig. 2 (b), the two nuclei are located in the same cavity. At this time, the orbitals remain molecular, and all the interaction

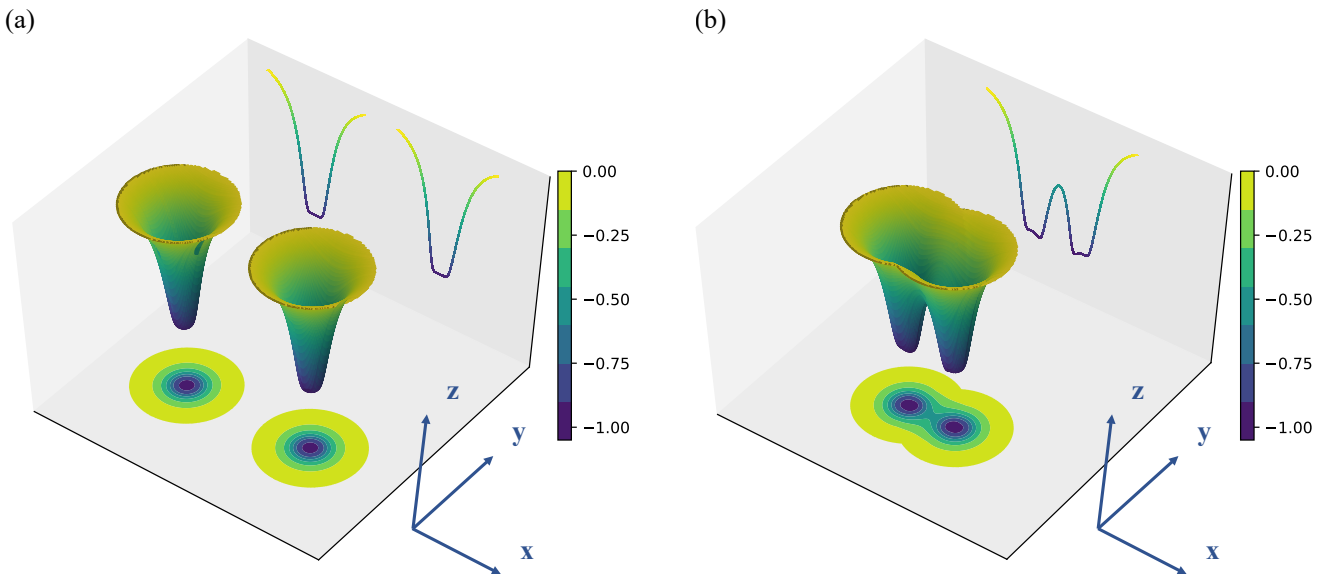


FIG. 2. (online color) *3D diagram of double potential well*. For quantum mechanically motion of nuclei, double potential well of the dissociative system is described in panel (a) when the distance between the nuclei is large (two nuclei are in different cavities), and well of the associative system are described in panel (b) when the distance between the nuclei is small (two nuclei are in the same cavity). For quantum mechanically motion of nuclei, the movement of the nucleus is instantaneous through the tunneling effect. For classical mechanically motion of nuclei, quantum tunneling will be banned, replaced by the slow movement of nuclei. For association process, two atomic nuclei move toward each other slowly (from (a) to (b)). For dissociation process, two atomic nuclei move in opposite directions slowly (from (b) to (a)).

forces involving atomic orbitals do not exist, that is, $g_{\Omega\uparrow,\downarrow,s} = 0$, and only the interaction forces $g_{\omega\uparrow,\downarrow}$ involving molecular orbitals are retained. Due to the instantaneous nature of the quantum tunneling effect (from panel (a) to panel (b) or from panel (b) to panel (a)), the change in the strength of the interaction force is instantaneous.

- **Classical motion of nuclei.** In this way, the movement of the nucleus is not instantaneous, but moves slowly. When the nuclei slowly approach, the whole system gradually develops from two independent atoms to a molecule. This process is accompanied by the interaction forces $g_{\Omega\uparrow,\downarrow,s}$ involving atomic orbitals gradually decreasing to 0, while the interaction forces $g_{\omega\uparrow,\downarrow}$ involving molecular orbitals gradually increases from 0. Conversely, when the nuclei slowly move away, the whole system gradually develops from a molecule to two independent atoms. This process is accompanied by the interaction forces $g_{\omega\uparrow,\downarrow}$ involving molecular orbitals gradually decreasing to 0, while the interaction forces $g_{\Omega\uparrow,\downarrow,s}$ involving atomic orbitals gradually increases from 0. The magnitude of the relative force is related to the distance between the nuclei, but what we are looking for is the time-dependent curves rather than the distance-dependent curves. We need to use time to find the distance and then find the magnitude of the interaction force. For conve-

nience, we can directly define the equation for the relationship between the magnitude of the relative force and the magnitude of the evolution time (in the laboratory, the speed of the nuclei can be controlled to satisfy this relationship). We define two types of relationships

$$g_{\Omega\uparrow,\downarrow,s}(t) = g_{\Omega\uparrow,\downarrow,s}^{max} \left(1 - \frac{t}{T}\right) \quad (16a)$$

$$g_{\omega\uparrow,\downarrow}(t) = g_{\omega\uparrow,\downarrow}^{max} \frac{t}{T} \quad (16b)$$

$$g_{\Omega\uparrow,\downarrow,s}(t) = g_{\Omega\uparrow,\downarrow,s}^{max} \left(\frac{\cos\left(\pi\frac{t}{T}\right) + 1}{2}\right) \quad (17a)$$

$$g_{\omega\uparrow,\downarrow}(t) = g_{\omega\uparrow,\downarrow}^{max} \left(\frac{\sin\left(\pi\frac{t}{T} - \frac{\pi}{2}\right) + 1}{2}\right) \quad (17b)$$

where T — the total time it takes to complete the evolution, $g_{\Omega\uparrow,\downarrow,s}^{max}$ is the maximum value of interaction forces $g_{\Omega\uparrow,\downarrow,s}(t)$ when the two nuclei are far enough apart that the system consists of two completely independent atoms, and $g_{\omega\uparrow,\downarrow}^{max}$ is the maximum value of interaction forces $g_{\omega\uparrow,\downarrow}(t)$ when the two nuclei are close enough that the system consists of one molecule. Eq. (16) is called straight-type relationship and Eq. (17) — trigonometric-type relationship. Eqs. (16) and (17) are defined for asso-

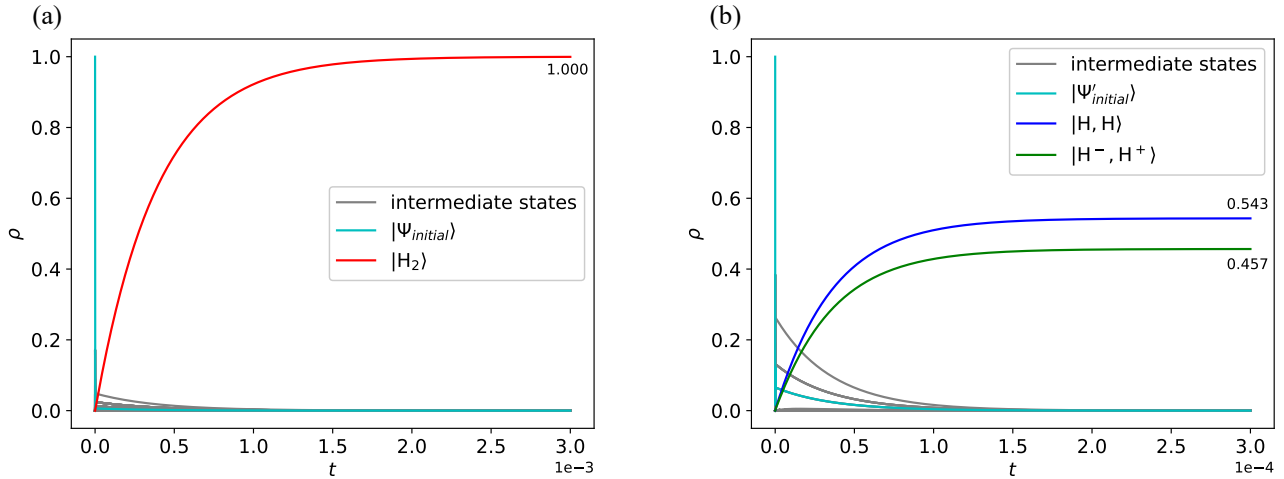


FIG. 3. (online color) *Quantum motion of nuclei*. Quantum tunneling is portrayed. Panel (a) shows the time-dependent curves of quantum states in association process with the initial condition of $|\Psi_{initial}\rangle$, which is depicted in Fig. 1 (d). Final state $|H_2\rangle$ is depicted in Fig. 1 (f). Panel (b) shows the time-dependent curves of quantum states in dissociation process with the initial condition of $|\Psi'_{initial}\rangle$, which is depicted in Fig. 1 (e). The final states that make up $|H, H\rangle$ and $|H^-, H^+\rangle$ are depicted in Fig. 5.

ciation process. Then, we define the corresponding equations for dissociation process as following

$$g_{\Omega\uparrow,\downarrow,s}(t) = g_{\Omega\uparrow,\downarrow,s}^{max} \frac{t}{T} \quad (18a)$$

$$g_{\omega\uparrow,\downarrow}(t) = g_{\omega\uparrow,\downarrow}^{max} \left(1 - \frac{t}{T}\right) \quad (18b)$$

$$g_{\Omega\uparrow,\downarrow,s}(t) = g_{\Omega\uparrow,\downarrow,s}^{max} \left(\frac{\sin\left(\pi\frac{t}{T} - \frac{\pi}{2}\right) + 1}{2} \right) \quad (19a)$$

$$g_{\omega\uparrow,\downarrow}(t) = g_{\omega\uparrow,\downarrow}^{max} \left(\frac{\cos\left(\pi\frac{t}{T}\right) + 1}{2} \right) \quad (19b)$$

III. NUMERICAL METHOD

The solution $\rho(t)$ in Eq. (10) may be approximately found as a sequence of two steps: in the first step we make one step in the solution of the unitary part of Eq. (10)

$$\tilde{\rho}(t+dt) = \exp\left(-\frac{i}{\hbar}Hdt\right)\rho(t)\exp\left(\frac{i}{\hbar}Hdt\right) \quad (20)$$

where we introduce PTSTM to compute the matrix exponential (see Appx. C). And in the second step, make one step in the solution of Eq. (10) with the commutator removed:

$$\rho(t+dt) = \tilde{\rho}(t+dt) + \frac{1}{\hbar}L(\tilde{\rho}(t+dt))dt \quad (21)$$

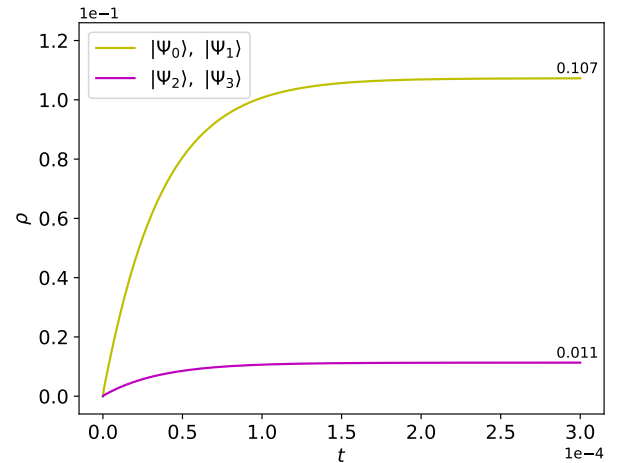


FIG. 4. (online color) *Dark states in the case of quantum motion of nuclei*. In the dissociation process, some dark states, exist in the form of singlet, are obtained: $|D_1\rangle = |\Psi_0\rangle - |\Psi_1\rangle$, $|D_2\rangle = |\Psi_2\rangle - |\Psi_3\rangle$.

IV. SIMULATIONS AND RESULTS

Different from previous work, in this paper, we study both the association and dissociation process of neutral hydrogen molecule. Thus, we consider two initial states:

- The initial state $|\Psi_{initial}\rangle$, shown in Fig. 1 (d), represents that the two nuclei are in different cavities, and the electrons are in the atomic ground state

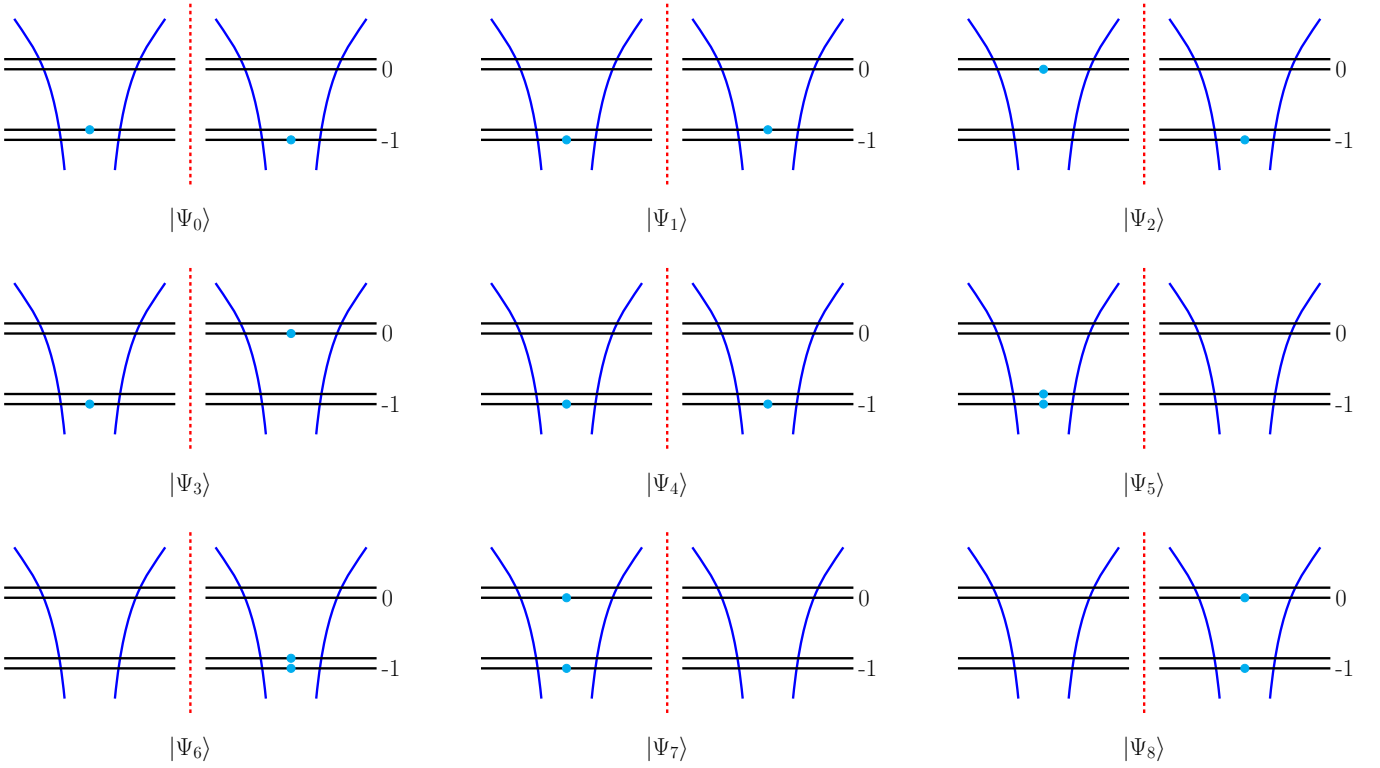


FIG. 5. (online color) *Nine final states in the case of dissociation process.* The nine states here can be clearly divided into two types based on the amount of charge: when each hydrogen atom carries one electron, they both are electrically neutral, thus, $|\Psi_0\rangle \sim |\Psi_4\rangle$ are uniformly expressed as $|\text{H}, \text{H}\rangle$; when both electrons are on the same hydrogen atom, at this time, one atom is electrically negative and the another is electrically positive, thus, $|\Psi_5\rangle \sim |\Psi_8\rangle$ are uniformly expressed as $|\text{H}^-, \text{H}^+\rangle$.

with spin down. We pump into two photons with different modes Ω^\uparrow and Ω^\downarrow . And a spin photon is also pumped in.

- The initial state $|\Psi'_{initial}\rangle$, shown in Fig. 1 (e), represents that the two nuclei are in the same cavity, and the electrons are in the molecular ground state with different spins. We only pump into two photons with different modes ω^\uparrow and ω^\downarrow .

A. Results of quantum motion of nuclei

In simulations: $\hbar = 1$, $\Omega^\uparrow = \Omega^\downarrow = 10^{10}$, $\omega^\uparrow = \omega^\downarrow = 5 * 10^9$, $\Omega^s = 10^9$; $g_{\Omega^\uparrow} = g_{\Omega^\downarrow} = 0.01 * \Omega^\uparrow$, $g_{\omega^\uparrow} = g_{\omega^\downarrow} = 0.01 * \omega^\uparrow$, $g_{\Omega^s} = 0.01 * \Omega^s$; $\zeta_2 = 10 * g_{\Omega^\uparrow}$, $\zeta_1 = g_{\Omega^\uparrow}$, $\zeta_0 = 0$; $\gamma_{\omega^\uparrow} = \gamma_{\omega^\downarrow} = \gamma_{\Omega^\uparrow} = \gamma_{\Omega^\downarrow} = \gamma_{\Omega^s} = 0.1 * g_{\Omega^\uparrow}$.

In Fig. 3, quantum mechanically motion of nuclei is considered. In panel 3 (a), the initial state is $|\Psi_{initial}\rangle$, described in Fig. 1 (d). In order to obtain the formation of hydrogen molecule, only the influx of photon with mode $\Omega^{\uparrow,\downarrow,s}$ is taken into account, and the influx of photons with modes $\omega^{\uparrow,\downarrow}$ is forbidden. And as stated in Sec. IIC, the influx rate is always lower than the corresponding dissipative rate. We assume that $\mu_{\Omega^{\uparrow,\downarrow,s}} = 0.5$, $\mu_{\omega^{\uparrow,\downarrow}} = 0$. According to numerical results

in Fig. 3 (a), we discovered that the red solid curve of state $|\text{H}_2\rangle$, described in Fig. 1 (f), climbs and reaches 1 at the end. It indicates that the formation of H_2 has been accomplished and that there are no longer any free hydrogen atoms. In order to force electrons to move from the molecular ground orbital to the excited orbital, the decomposition of hydrogen molecules must absorb photons with mode $\omega^{\uparrow,\downarrow}$, but because these photons cannot be replenished, they will gradually leak until they are completely absent in the cavity. As a result, the system finally evolves over time to generate a stable neutral hydrogen molecule.

In panel 3 (b), the initial state is $|\Psi'_{initial}\rangle$, described in Fig. 1 (e). In order to obtain the decomposition of hydrogen molecule, only the influx of photon with mode $\omega^{\uparrow,\downarrow}$ is taken into account, and the influx of photons with modes $\Omega^{\uparrow,\downarrow,s}$ is forbidden. We assume that $\mu_{\Omega^{\uparrow,\downarrow,s}} = 0$, $\mu_{\omega^{\uparrow,\downarrow}} = 0.5$. According to numerical results in Fig. 3 (b), we discovered that the blue solid curve of state $|\text{H}, \text{H}\rangle$ climbs and reaches 0.543 and the green solid curve of state $|\text{H}^-, \text{H}^+\rangle$ climbs and reaches 0.457 at the end. Final state $|\text{H}, \text{H}\rangle$, indicating that each atom is neutrally charged, consists of $|\Psi_0\rangle \sim |\Psi_4\rangle$. And final state $|\text{H}^-, \text{H}^+\rangle$, indicating that one atom is negatively charged and the other is positively charged, consists of $|\Psi_5\rangle \sim |\Psi_8\rangle$. $|\Psi_0\rangle \sim |\Psi_8\rangle$ are all described in Fig. 5. It

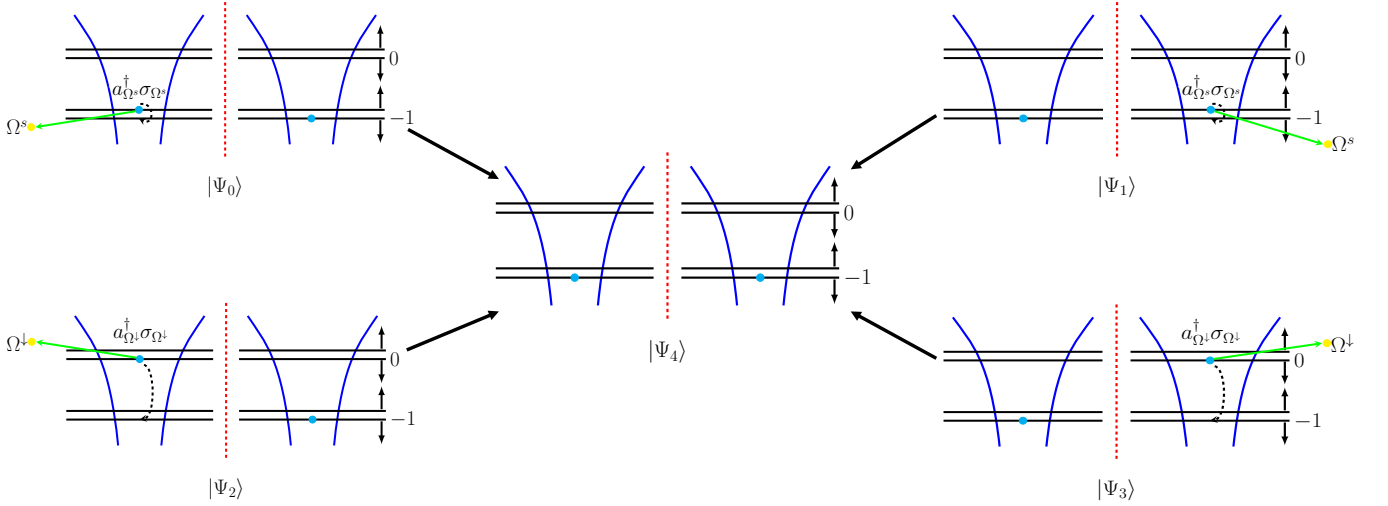


FIG. 6. (online color) *Two combinations of dark states.* Here we can see that for $|\Psi_0\rangle$ and $|\Psi_1\rangle$, under the action of $a_{\Omega^s}^\dagger \sigma_{\Omega^s}$, the upspin electrons on the ground state are simultaneously flipped to downspin to obtain $|\Psi_4\rangle$ respectively, and then the two states $|\Psi_4\rangle$ cancel out under the action of subtraction. Therefore $|D_1\rangle$ is a singlet. Same reason that for $|\Psi_2\rangle$ and $|\Psi_3\rangle$, under the action of $a_{\Omega^\downarrow}^\dagger \sigma_{\Omega^\downarrow}$, the electrons on the excited state are simultaneously flipped to ground state to obtain $|\Psi_4\rangle$ respectively, and then the two states $|\Psi_4\rangle$ cancel out, too. Therefore $|D_2\rangle$ is also a singlet.

indicates that the decomposition of H_2 has been obtained and that there are no longer stable hydrogen molecule. In order to force electrons to move from the atomic ground orbital to the excited orbital, the formation of hydrogen molecules must absorb photons with mode $\Omega^{\uparrow,\downarrow,s}$, but because these photons cannot be replenished, they will gradually leak until they are completely absent in the cavity. As a result, the system finally evolves over time to generate two independent hydrogen atoms. Obviously, it can be concluded from the Fig. 5 that the reason why the blue and green solid curves do not overlap is that the two states $|\text{H}, \text{H}\rangle$ and $|\text{H}^-, \text{H}^+\rangle$ are asymmetric.

During the disintegration of hydrogen molecule, two dark state combinations (two singlets) appear

$$|D_1\rangle = c_1 (|\Psi_0\rangle - |\Psi_1\rangle) \quad (22a)$$

$$|D_2\rangle = c_2 (|\Psi_2\rangle - |\Psi_3\rangle) \quad (22b)$$

where c_1 , c_2 are normalization factor. The formation mechanism of these two dark states is shown in Fig. 6, and we have

$$\begin{aligned} a_{\Omega^s}^\dagger \sigma_{\Omega^s} |D_1\rangle &= c_1 a_{\Omega^s}^\dagger \sigma_{\Omega^s} (|\Psi_0\rangle - |\Psi_1\rangle) \\ &= c_1 (a_{\Omega^s}^\dagger \sigma_{\Omega^s} |\Psi_0\rangle - a_{\Omega^s}^\dagger \sigma_{\Omega^s} |\Psi_1\rangle) \\ &= c_1 (|\Psi_4\rangle - |\Psi_4\rangle) \\ &= 0 \end{aligned} \quad (23a)$$

$$\begin{aligned} a_{\Omega^\downarrow}^\dagger \sigma_{\Omega^\downarrow} |D_2\rangle &= c_2 a_{\Omega^\downarrow}^\dagger \sigma_{\Omega^\downarrow} (|\Psi_2\rangle - |\Psi_3\rangle) \\ &= c_2 (a_{\Omega^\downarrow}^\dagger \sigma_{\Omega^\downarrow} |\Psi_2\rangle - a_{\Omega^\downarrow}^\dagger \sigma_{\Omega^\downarrow} |\Psi_3\rangle) \\ &= c_2 (|\Psi_4\rangle - |\Psi_4\rangle) \\ &= 0 \end{aligned} \quad (23b)$$

where $\sigma_{\Omega^s} = \sigma_{\Omega^s,1} + \sigma_{\Omega^s,2}$ and $\sigma_{\Omega^\downarrow} = \sigma_{\Omega^\downarrow,1} + \sigma_{\Omega^\downarrow,2}$

B. Results of classical motion of nuclei

Except for interaction forces, other parameters are the same as in Sec. IV A.

In Fig. 7, classical mechanically motion of nuclei is considered. In panel 7 (a), the initial state is also $|\Psi_{initial}\rangle$. For association process, we consider two definitions of interaction forces: the first is straight-type relationship, described in Eq. (16); the second is trigonometric-type relationship, described in Eq. (17). We assume that $\mu_{\Omega^{\uparrow,\downarrow,s}} = 0.5$, $\mu_{\omega^{\uparrow,\downarrow}} = 0$. According to numerical results in Fig. 7 (a), we discovered that the red solid and red dashed curves of state $|\text{H}_2\rangle$ climb and reach almost 1 at the end. Although the two curves do not overlap, they both reach the same value in the end. Moreover, when the interaction forces satisfy the straight-type relationship, the curve climbs faster.

In panel 7 (b), the initial state is also $|\Psi'_{initial}\rangle$. For dissociation process, we consider two definitions of interaction forces: the first is straight-type relationship, described in Eq. (18); the second is trigonometric-type relationship, described in Eq. (19). We assume that $\mu_{\Omega^{\uparrow,\downarrow,s}} = 0$, $\mu_{\omega^{\uparrow,\downarrow}} = 0.5$. In Fig. 7 (b), we discovered that the blue solid and blue dashed curves of state $|\text{H}, \text{H}\rangle$ climb and reach the same value and the green solid and green dashed curves of state $|\text{H}^-, \text{H}^+\rangle$ climb and reach also the same value at the end. Same as Fig. 7 (a), when the interaction forces satisfy the straight-type relationship, the curve climbs faster. The curves of dark states under the case of classical motion are shown in Fig. 8.

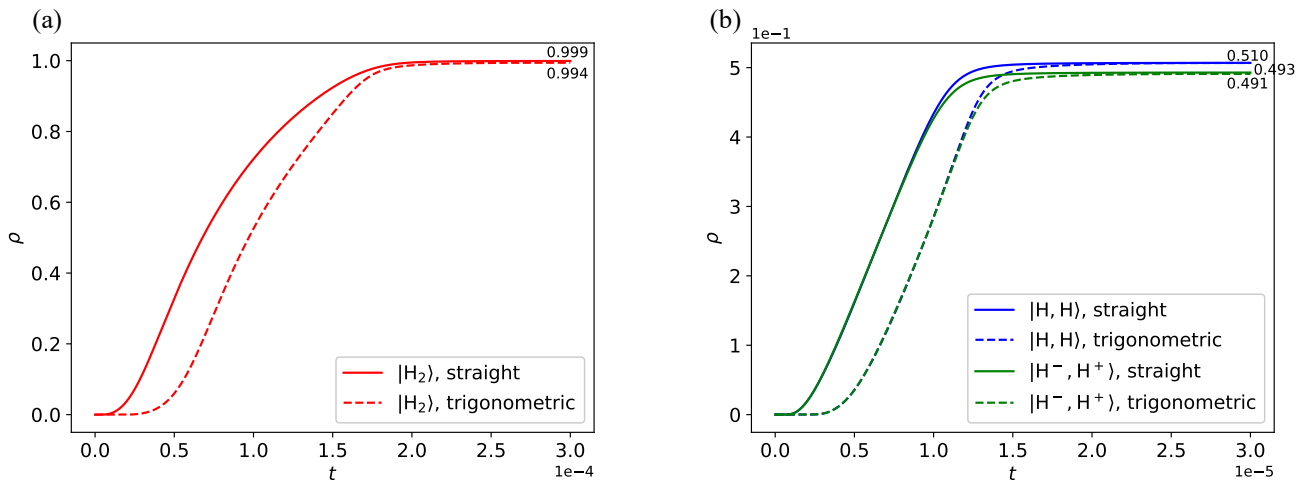


FIG. 7. (online color) *Classical motion of nuclei*. Quantum tunneling is forbidden, replaced by slow motion of nuclei. The solid curves correspond to the straight-type fluctuation of the interactions, and the dashed curves correspond to the trigonometric-type fluctuation. Same as Fig. 3, association and dissociation processes with different initial states are shown in panels (a) and (b), respectively.

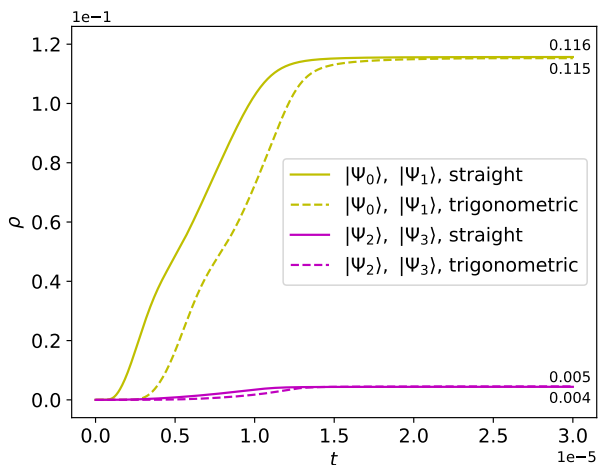


FIG. 8. (online color) *Dark states in the case of classical motion of nuclei*. Same as Fig. 4, two singlets $|D_1\rangle$ and $|D_2\rangle$ are obtained.

V. CONCLUDING DISCUSSION AND FUTURE WORK

In this paper, we simulate both the association and dissociation of the neutral hydrogen molecule with different

initial conditions. The theoretical model has been constructed, and several analytical findings have been drawn from it: In Sec. IV, comparing quantum and classical mechanically motion of nuclei, we will find that the time required to obtain the final states ($|H_2\rangle$, $|H, H\rangle$, $|H^-, H^+\rangle$) under the case of classical motion is one order of magnitude smaller than that under the case of quantum motion. In addition, the slope of the curves of the final states under the case of quantum motion is firstly large and then small, while the slope of the curves under the case of classical motion is firstly small, then large, and finally small. We also found two dark state combinations $|D_1\rangle$ and $|D_2\rangle$ during the dissociation process.

Although our approach is still imperfect, it has the advantages of being simple and scalable. This article is a supplement and expansion of previous work [7, 8]. The results obtained make the study of the association-dissociation model of neutral hydrogen molecule more comprehensive, and also lay the foundation for the study of more intricate chemical and biologic models.

ACKNOWLEDGMENTS

This work was supported by the China Scholarship Council (CSC No.202108090483).

Appendix A: Rotating wave approximation

RWA is taken into account in this paper. When the strength of the applied electromagnetic radiation is close to resonance with an atomic transition and the strength is low, this approximation holds true [53]. Thus,

$$\frac{g}{\hbar\omega_{cavity}} \approx \frac{g}{\hbar\omega_{atom}} \ll 1 \quad (\text{A1})$$

where ω_{cavity} stands for cavity frequency and ω_{atom} for transition frequency (of atom). RWA allows us to change $(\sigma^\dagger + \sigma)(a^\dagger + a)$ to $\sigma^\dagger a + \sigma a^\dagger$. In Sec. II A we typically presume that $\Omega_{cavity} = \Omega_{atom}$.

Appendix B: Operators

On a p -photons state, the photon annihilation and creation operators are described as

$$\begin{aligned} \text{if } p > 0, & \begin{cases} a|p\rangle = \sqrt{p}|p-1\rangle, \\ a^\dagger|p\rangle = \sqrt{p+1}|p+1\rangle, \end{cases} \\ \text{if } p = 0, & \begin{cases} a|0\rangle = 0, \\ a^\dagger|0\rangle = |1\rangle. \end{cases} \end{aligned} \quad (\text{B1})$$

Operators $a_{\Omega^\uparrow, \downarrow, s}$, $a_{\omega^\uparrow, \downarrow}$ and their conjugate operators all obey this rule. The interaction of molecule with the electromagnetic field of the cavity, emitting or absorbing photon with mode $\omega^\uparrow, \downarrow$, is described as

$$\begin{aligned} \sigma_{\omega^\uparrow, \downarrow} |1\rangle_{\Phi_1}^\uparrow, \downarrow |0\rangle_{\Phi_0}^\uparrow, \downarrow &= |0\rangle_{\Phi_1}^\uparrow, \downarrow |1\rangle_{\Phi_0}^\uparrow, \downarrow, \\ \sigma_{\omega^\uparrow, \downarrow}^\dagger |0\rangle_{\Phi_1}^\uparrow, \downarrow |1\rangle_{\Phi_0}^\uparrow, \downarrow &= |1\rangle_{\Phi_1}^\uparrow, \downarrow |0\rangle_{\Phi_0}^\uparrow, \downarrow. \end{aligned} \quad (\text{B2})$$

The interaction of atom with the electromagnetic field, emitting or absorbing photon with mode $\Omega^\uparrow, \downarrow$, is described as

$$\begin{aligned} \sigma_{\Omega^\uparrow, \downarrow, i} |1\rangle_{at_i}^\uparrow, \downarrow |0\rangle_{or_{-1}}^\uparrow, \downarrow &= |0\rangle_{at_i}^\uparrow, \downarrow |1\rangle_{or_{-1}}^\uparrow, \downarrow, \\ \sigma_{\Omega^\uparrow, \downarrow, i}^\dagger |0\rangle_{at_i}^\uparrow, \downarrow |1\rangle_{or_{-1}}^\uparrow, \downarrow &= |1\rangle_{at_i}^\uparrow, \downarrow |0\rangle_{or_{-1}}^\uparrow, \downarrow. \end{aligned} \quad (\text{B3})$$

The interaction of atom with the electromagnetic field, emitting or absorbing photon with mode Ω^s , is described as

$$\begin{aligned} \sigma_{\Omega^s, i} |1\rangle_{or_0}^\uparrow |0\rangle_{at_i}^\downarrow &= |0\rangle_{at_i}^\uparrow |1\rangle_{or_0}^\downarrow, \\ \sigma_{\Omega^s, i} |1\rangle_{or_{-1}}^\uparrow |0\rangle_{at_i}^\downarrow &= |0\rangle_{or_{-1}}^\uparrow |1\rangle_{at_i}^\downarrow, \\ \sigma_{\Omega^s, i}^\dagger |0\rangle_{or_0}^\uparrow |1\rangle_{at_i}^\downarrow &= |1\rangle_{or_0}^\uparrow |0\rangle_{at_i}^\downarrow, \\ \sigma_{\Omega^s, i}^\dagger |0\rangle_{or_{-1}}^\uparrow |1\rangle_{at_i}^\downarrow &= |1\rangle_{or_{-1}}^\uparrow |0\rangle_{at_i}^\downarrow. \end{aligned} \quad (\text{B4})$$

The nuclei's tunnelling operators, $\sigma_n, \sigma_n^\dagger$, have following form

$$\begin{aligned} \sigma_n |1\rangle_n &= |0\rangle_n, \\ \sigma_n^\dagger |0\rangle_n &= |1\rangle_n. \end{aligned} \quad (\text{B5})$$

Appendix C: Precise time step integration method

For decades, a dozen different ways to compute the matrix exponential have been examined [54, 55]. However, the exponential problem has not yet been fully resolved illustrates how important it is. PTSIM of matrix exponential was proposed in 1991 [56] and has been developed over the decades since then [57–60]. This method avoids computer truncation errors caused by fine division and improves the numerical solution of matrix exponential to computer

accuracy. When solving the equations of motion using stepwise integration, the matrix exponential operation involved is $e^{A\Delta t}$. According to the addition theorem of matrix exponential

$$e^{A\Delta t} = \left[e^{A\frac{\Delta t}{2^N}} \right]^{2^N} = [e^{A\varepsilon}]^{2^N} \quad (\text{C1})$$

where A is matrix, Δt is time step, $\varepsilon = \frac{\Delta t}{2^N}$ (usually N is taken to be equal to 20). The matrix exponential can be approximated using Taylor series expansion (4 terms)

$$e^{A\varepsilon} \approx I + A\varepsilon + \frac{(A\varepsilon)^2}{2!} + \frac{(A\varepsilon)^3}{3!} + \frac{(A\varepsilon)^4}{4!} \quad (\text{C2})$$

where I is unit matrix, then

$$\begin{aligned} e^{A\Delta t} &\approx \left[I + A\varepsilon + \frac{(A\varepsilon)^2}{2!} + \frac{(A\varepsilon)^3}{3!} + \frac{(A\varepsilon)^4}{4!} \right]^{2^N} \\ &= [I + T_{a,0}]^{2^N} \end{aligned} \quad (\text{C3})$$

where $T_{a,0} = A\varepsilon + \frac{(A\varepsilon)^2}{2!} + \frac{(A\varepsilon)^3}{3!} + \frac{(A\varepsilon)^4}{4!}$, then

$$[I + T_{a,0}]^{2^N} = [I + 2T_{a,0} + T_{a,0}T_{a,0}]^{2^{N-1}} = [I + T_{a,1}]^{2^{N-1}} = [I + T_{a,2}]^{2^{N-2}} = \cdots = [I + T_{a,N}] \quad (\text{C4})$$

where $T_{a,n} = 2T_{a,n-1} + T_{a,n-1}T_{a,n-1}$, $n \geq 1$.

-
- [1] J. Zhu, Quantum simulation of dissociative ionization of H_2^+ in full dimensionality with a time-dependent surface-flux method, *Phys. Rev. A* **102**, 053109 (2020).
- [2] A. Vitaliy, K. Zheng, K. Alexei, H. Miao, O. Yuri, L. Wanshun, and V. Nadezda, About chemical modifications of finite dimensional QED models, *Nonlinear Phenomena in Complex Systems* **24**, 230 (2021).
- [3] Q. Wang, H.-Y. Liu, Q.-S. Li, Y. Li, Y. Chai, Q. Gong, H. Wang, Y.-C. Wu, Y.-J. Han, G.-C. Guo, and G.-P. Guo, ChemiQ: A chemistry simulator for quantum computer (2021).
- [4] J. R. McClean, N. C. Rubin, J. Lee, M. P. Harrigan, T. E. O'Brien, R. Babbush, W. J. Huggins, and H.-Y. Huang, What the foundations of quantum computer science teach us about chemistry, *The Journal of Chemical Physics* **155**, 150901 (2021).
- [5] D. Claudino, A. J. McCaskey, and D. I. Lyakh, A backend-agnostic, quantum-classical framework for simulations of chemistry in C++, *ACM Transactions on Quantum Computing* **4**, 10.1145/3523285 (2022).
- [6] R. Chen, J. You, and Y. I. Ozhigov, Qualitative model of the hydrogen peroxide positive ion in a heat bath, *Comput Math Model* **33**, 408 (2022).
- [7] H. hui Miao and Y. I. Ozhigov, Using a modified version of the Tavis-Cummings-Hubbard model to simulate the formation of neutral hydrogen molecule, *Physica A: Statistical Mechanics and its Applications* **622**, 128851 (2023).
- [8] H.-h. Miao and Y. I. Ozhigov, Comparing the effects of nuclear and electron spins on the formation of neutral hydrogen molecule, *Lobachevskii Journal of Mathematics* **44**, 3111 (2023).
- [9] H. hui Miao, Investigating entropic dynamics of multiqubit cavity QED system (2024), arXiv:2405.05696 [quant-ph].
- [10] I. I. Rabi, On the process of space quantization, *Phys. Rev.* **49**, 324 (1936).
- [11] I. I. Rabi, Space quantization in a gyrating magnetic field, *Phys. Rev.* **51**, 652 (1937).
- [12] R. H. Dicke, Coherence in spontaneous radiation processes, *Phys. Rev.* **93**, 99 (1954).
- [13] J. J. Hopfield, Theory of the contribution of excitons to the complex dielectric constant of crystals, *Phys. Rev.* **112**, 1555 (1958).
- [14] E. Jaynes and F. Cummings, Comparison of quantum and semiclassical radiation theories with application to the beam maser, *Proceedings of the IEEE* **51**, 89 (1963).
- [15] M. Tavis and F. W. Cummings, Exact solution for an N -molecule—radiation-field Hamiltonian, *Phys. Rev.* **170**, 379 (1968).
- [16] J. Casanova, G. Romero, I. Lizuain, J. J. García-Ripoll, and E. Solano, Deep strong coupling regime of the Jaynes-Cummings model, *Phys. Rev. Lett.* **105**, 263603 (2010).
- [17] S. Haroche, Nobel lecture: Controlling photons in a box and exploring the quantum to classical boundary, *Rev. Mod. Phys.* **85**, 1083 (2013).
- [18] X. Gu, A. F. Kockum, A. Miranowicz, Y. xi Liu, and F. Nori, Microwave photonics with superconducting quantum circuits, *Physics Reports* **718-719**, 1 (2017), microwave photonics with superconducting quantum circuits.
- [19] P. Forn-Díaz, L. Lamata, E. Rico, J. Kono, and E. Solano, Ultrastrong coupling regimes of light-matter interaction, *Rev. Mod. Phys.* **91**, 025005 (2019).
- [20] A. F. Kockum and F. Nori, Quantum bits with Josephson junctions, in *Fundamentals and Frontiers of the Josephson Effect*, edited by F. Tafuri (Springer International

- Publishing, Cham, 2019) pp. 703–741.
- [21] A. Frisk Kockum, A. Miranowicz, S. De Liberato, S. Savasta, and F. Nori, Ultrastrong coupling between light and matter, *Nature Reviews Physics* **1**, 19 (2019).
- [22] D. G. Angelakis, M. F. Santos, and S. Bose, Photon-blockade-induced mott transitions and XY spin models in coupled cavity arrays, *Phys. Rev. A* **76**, 031805 (2007).
- [23] S. Prasad and A. Martin, Effective three-body interactions in Jaynes–Cummings–Hubbard systems, *Sci Rep* **8**, 16253 (2018).
- [24] H. Wei, J. Zhang, S. Greschner, T. C. Scott, and W. Zhang, Quantum monte carlo study of superradiant supersolid of light in the extended Jaynes–Cummings–Hubbard model, *Phys. Rev. B* **103**, 184501 (2021).
- [25] K. C. Smith, A. Bhattacharya, and D. J. Masiello, Exact k -body representation of the Jaynes–Cummings interaction in the dressed basis: Insight into many-body phenomena with light, *Phys. Rev. A* **104**, 013707 (2021).
- [26] Y. Ozhigov, Quantum gates on asynchronous atomic excitations, *Quantum Electron.* **50**, 10.1070/QEL17320 (2020).
- [27] R. Düll, A. Kulagin, L. Lee, Y. Ozhigov, H. Miao, and K. Zheng, Quality of control in the Tavis–Cummings–Hubbard model, *Computational Mathematics and Modeling* **32**, 75 (2021).
- [28] H. hui Miao, Investigating entropic dynamics of multi-qubit cavity QED system (2024).
- [29] H. hui Miao and W. Li, Entanglement and quantum discord in the cavity QED model (2024).
- [30] E. S. Lee, C. Geckeler, J. Heurich, A. Gupta, K.-I. Cheong, S. Secrest, and P. Meystre, Dark states of dressed bose-einstein condensates, *Phys. Rev. A* **60**, 4006 (1999).
- [31] P. Kok, K. Nemoto, and W. J. Munro, Properties of multi-partite dark states (2002).
- [32] A. André, L.-M. Duan, and M. D. Lukin, Coherent atom interactions mediated by dark-state polaritons, *Phys Rev Lett* **88**, 243602 (2002).
- [33] C. Pörtl, C. Emary, and T. Brandes, Spin entangled two-particle dark state in quantum transport through coupled quantum dots, *Physical Review B* **87** (2012).
- [34] T. Tanamoto, K. Ono, and F. Nori, Steady-state solution for dark states using a three-level system in coupled quantum dots, *Japanese Journal of Applied Physics* **51**, 02BJ07 (2012).
- [35] J. Hansom, C. H. H. Schulte, C. Le Gall, C. Matthiesen, E. Clarke, M. Hugues, J. M. Taylor, and M. Atatüre, Environment-assisted quantum control of a solid-state spin via coherent dark states, *Nature Physics* **10**, 725 (2014).
- [36] S. V. Kozyrev and I. V. Volovich, Dark states in quantum photosynthesis (2016).
- [37] Y. I. Ozhigov, Space of dark states in Tavis–Cummings model, *Modern Information Technologies and IT Education* **15**, 27 (2019).
- [38] A. V. Kulagin and Y. I. Ozhigov, Optical selection of dark states of multilevel atomic ensembles, *Computational Mathematics and Modeling* **31**, 431 (2020).
- [39] L. Guo, S. Greschner, S. Zhu, and W. Zhang, Supersolid and pair correlations of the extended Jaynes–Cummings–Hubbard model on triangular lattices, *Phys. Rev. A* **100**, 033614 (2019).
- [40] N. Victorova, A. Kulagin, and Y. Ozhigov, Quasi-classical description of the “quantum bottleneck” effect for thermal relaxation of an atom in a resonator, *Comput Math Model* **31**, 1 (2020).
- [41] A. Kulagin and Y. Ozhigov, Realization of grover search algorithm on the optical cavities, *Lobachevskii J Math* **43**, 864 (2022).
- [42] V. Afanasyev, C. Ran, Y. Ozhigov, and Y. Jiangchuan, Collapse of dark states in Tavis–Cummings model, *arXiv preprint arXiv:2207.03175* (2022).
- [43] Y. Ozhigov and I. Pluzhnikov, Superimposition and antagonism in chain synthesis using entangled biphotonic control, *Comput Math Model* **33**, 24 (2022).
- [44] H. hui Miao and Y. I. Ozhigov, Distributed computing quantum unitary evolution (2024).
- [45] W. Li, H. hui Miao, and Y. I. Ozhigov, Supercomputer model of finite-dimensional quantum electrodynamics applications (2024).
- [46] R. Alicki, The quantum open system as a model of the heat engine, *Journal of Physics A: Mathematical and General* **12**, L103 (1979).
- [47] H.-P. Breuer, F. Petruccione, *et al.*, *The theory of open quantum systems* (Oxford University Press, 2002).
- [48] R. Kosloff, Quantum thermodynamics: A dynamical viewpoint, *Entropy* **15**, 2100 (2013).
- [49] W. Pauli, Über den Zusammenhang des Abschlusses der Elektronengruppen im Atom mit der Komplexstruktur der Spektren, *Zeitschrift für Physik* **31**, 765 (1925).
- [50] P. A. M. Dirac, The quantum theory of the emission and absorption of radiation, *Proc. R. Soc. A* , 243 (1927).
- [51] V. Fock, Konfigurationsraum und zweite quantelung, *Zeitschrift für Physik* **75**, 622 (1932).
- [52] A. Kulagin, V. Ladunov, Y. Ozhigov, N. Skovoroda, and N. Victorova, Homogeneous atomic ensembles and single-mode field: review of simulation results, in *International Conference on Micro-and Nano-Electronics 2018*, Vol. 11022 (SPIE, 2019) pp. 600–611.
- [53] Y. Wu and X. Yang, Strong-coupling theory of periodically driven two-level systems, *Phys. Rev. Lett.* **98**, 013601 (2007).
- [54] C. Moler and C. Van Loan, Nineteen dubious ways to compute the exponential of a matrix, *SIAM Review* **20**, 801 (1978).
- [55] C. Moler and C. Van Loan, Nineteen dubious ways to compute the exponential of a matrix, twenty-five years later, *SIAM Review* **45**, 3 (2003).
- [56] W.-x. Zhong and Z.-s. Yang, On the computation of the main eigen-pairs of the continuous-time linear quadratic control problem, *Applied Mathematics and Mechanics* **12**, 45 (1991).
- [57] Z. W X and W. F W, A precise time step integration method, *Proceedings of the Institution of Mechanical Engineers, Part C: Journal of Mechanical Engineering Science* **208**, 427 (1994).
- [58] W.-x. Zhong, On precise time-integration method for structural dynamics, *Journal of Dalian University of Technology* **34**, 131 (1994).
- [59] W.-x. Zhong, Precise integration for transient analysis, *Computational Structure Mechanics and Applications* **12**, 1 (1995).
- [60] G. Qiang, T. ShuJun, and Z. WanXie, A survey of the precise integration method, *SCIENTIA SINICA Technologica* **46**, 1207 (2016).